KERNFORSCHUNGSZENTRUM

KARLSRUHE

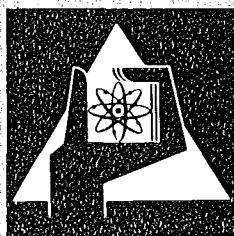August 1974

KFK 1951

Total Capture Cross Section of ^{59}Co
in the Neutron Energy Region 6 – 200 keV

Robert R. Spencer, H. Beer

KERNFORSCHUNGSZENTRUM KARLSRUHE

KFK 1951

Institut für Angewandte Kernphysik

Projekt Schneller Brüter

TOTAL CAPTURE CROSS SECTION OF ^{59}Co

IN THE NEUTRON ENERGY REGION 6-200 keV

Robert R. Spencer and H. Beer

ABSTRACT

The neutron capture cross section of ^{59}Co has been measured
in the energy range from 6 - 200 keV using an 800 ℓ liquid scintillator
detector in conjunction with a pulsed, 3 MV Van de Graaff. The
excellent time resolution of the system (FWHM = 2.8 ns) permitted deri-
vation of radiation widths for single s-wave resonances to 50 keV
neutron energy. Average radiation widths of 0.564 $\pm$ 0.024 eV and
0.486 $\pm$ 0.016 eV were found for seven J = 3 resonances and ten J = 4
resonances, respectively. No significant correlation between Γ_n^o and Γ_γ
was found for either spin state. The Maxwellian averaged cross section
for kT = 30 keV was found to be 72 mb over the region from thermal
to 200 keV neutron energy.

DER TOTALE EINFANGQUERSCHNITT VON ^{59}Co IM NEUTRONENENERGIEBEREICH 6-200 keV

ZUSAMMENFASSUNG

Der totale Neutronenwirkungsquerschnitt von ^{59}Co wurde im
Energiebereich 6 - 200 keV mit einem 800 ℓ Flüssigszintillator-Detek-
tor in Verbindung mit einem gepulsten 3 MV Van de Graaff gemessen.
Die ausgezeichnete Zeitauflösung der Anordnung (FWHM = 2,8 ns) ermög-
lichte die Bestimmung der Strahlungsbreiten einzelner s-Wellen Resonanzen
bis zu 50 keV Neutronenenergie. Für sieben Zustände mit J = 3 und zehn
Zuständen mit J = 4 wurden die mittleren Strahlungsbreiten zu 0.564
$\pm$ 0.024 eV bzw. 0.486 $\pm$ 0.016 eV bestimmt. Bei beiden Spinzuständen ergab
sich keine signifikante Korrelation zwischen Γ_n^o und Γ_γ. Der über eine
Maxwellverteilung mit kT = 30 keV im Bereich zwischen thermischen Energien
und 200 keV gemittelte Querschnitt wurde zu 72 mb berechnet.

1. INTRODUCTION

The neutron total capture cross section of ^{59}Co has been measured in the energy region from 6 to 200 keV using the Karlsruhe, pulsed 3 MV Van de Graaff and large liquid scintillation tank. This measurement was carried out in a continuing effort to obtain improved neutron capture and total cross sections of elements important to the fast breeder reactor project. Recent requests for capture cross sections of reactor structural materials ask for accuracies of $\pm$ 10 % or better. It has been clear that in order to achieve such accuracies, improvements must be made in several areas of the experimental technique. The most important of these are background determination, knowledge of the sensitivity of the gamma detector to sample scattered neutrons, and knowledge of the detector efficiency. It was felt that at least a part of these objectives could be attained by improvements in the detector performance. Therefore the Karlsruhe tank was recently renovated and a ^{6}Li liner was installed. The result was a marked improvement in both pulse height and time resolution and a reduced sensitivity to sample scattered neutrons, which made possible an accuracy approaching the desired $\pm$ 10 % for the capture measurements on ^{59}Co.

Knowledge of the capture cross section permits the determination of radiation widths for resonances whose spin and neutron width are known from analysis of total cross section measurements. Resonance parameters from high resolution total cross section data on ^{59}Co have been reported by Garg, et al. (1) and Morgenstern, et al. (2). Precise identification of corresponding resonances in the capture and total cross sections was made possible by the excellent energy agreement observed between the present data and those of references (1) and (2). This agreement and the present resolution permitted derivation of radiation widths for individual resonances from the lowest neutron energy of 6 keV to as high as 50 keV.

2. EXPERIMENTAL DESCRIPTIONS

2.1 Neutron Production

Neutrons were produced by means of the ^{7}Li(p,n)^{7}Be reaction with the proton beam pulsed at a 500 kHz repetition rate. The proton pulse width from the accelerator was 1 ns; however, due to the geometry of the beam transport system to the tank flight station,

the width was degraded somewhat to an estimated 1.5 ns. Neutrons at 0° to the incident proton beam were well collimated and impinged on the sample located in the center of the γ-ray detector after traversing a flight path of 2.03 meters. The primary run was taken with a relatively thick ($\simeq$ 100 keV) lithium target and a proton energy such that neutrons from a few keV to 200 keV were produced. A second run was taken at a proton energy which yielded 70 keV maximum neutron energy and, due to kinematics, no neutrons below about 8 keV. In this way the effect of over-lap neutrons in the primary run was found to be essentially negligable.

2.2 Gamma-ray Detector System

The Karlsruhe tank (3) is approximately 1.1 meter diameter, contains approximately 800 liters of liquid scintillator and has a 10 cm diameter, thin walled,aluminum through tube for placement of the sample at the tank center. The scintillator is viewed by twelve photomultipliers. Using 57 AVP photomultipliers Kompe (3) reported a pulse height resolution of 25 % for the 2.5 MeV ^{60}Co sum peak and measured a time resolution of 3 ns with the 1 ns pulsed proton beam striking a tantalum target at the sample position within the tank. In capture experiments, however, time resolutions of the order of 4-5 ns were common.

Recently, the tank was drained, sandblasted, repainted with reflec-tor material, and refitted with faster photomultipliers (60 DVP). A 2 cm thick ^{6}Li and moderator liner was installed around the aluminum through tube and new scintillator $^{+)}$ with 20 liters of tri-methyl borate was introduced. Slow pulses developed from the photomultiplier 10 th dynodes were used for pulse height analysis after matching and summing. Fast pulses from the anodes, carefully matched in pulse height and time, were summed and used for time analysis. A standard, fast-slow coincidence system correlated the pulses from the two branches for presentation to the on-line computer. Data were stored for each sample in a 1024 channel (time) by 12 channel (pulse height) array on both an interactive disc and a passive magnetic tape system.

$^{+)}$Nuclear Enterprises NE 224

Reduction of the effect of sample scattered neutrons by the ^{6}Li
liner and tri-methyl borate allowed a lower pulse height threshold
equivalent to 2 MeV γ-ray energy to be used. The detector system exhi-
bited a pulse height resolution of 18 % on the 2.5 MeV sum peak from
a ^{60}Co source placed at the center of the tank. During a 36 hour
period of the primary run, a time resolution of approximately 2.25 ns
(FWHM) was observed. Three such periods, comprising the full run,
showed significant base line and gain shifts in the timing system such
that a final resolution of approximately 2.8 ns resulted. With appropriate
stabilization, the system should be capable of achieving a time resolution
of 2 ns or less using a proton burst width of 1 ns.

2.3 Samples

Samples consisted of 90 mm ∅ by 1 mm thick metallic discs of 99.9 %
purity cobalt and gold and a similar graphite disc for background deter-
mination. The thickness of the graphite was chosen to match the "hard sphere"
scattering of ^{59}Co. The cobalt and gold sample thicknesses in nuclei per
barn were 0.0090 and 0.0058, respectively. An automatic sample changer cycled
the samples into the detector at approximately 15 minute intervals in order
to average out beam fluctuations. The exact cycling time was determined by
the proton beam integrator.

3. DATA AND ANALYSIS

3.1 Background

A detailed accounting for a number of different types of background
is essential when accurate values of capture cross sections are required.
Since reactor engineering requests are now for more precise values than
previously, it is necessary to improve the experimental determination and
each phase of the data accumulation must be examined carefully. Table I
gives a break-down of the large scintillator background into categories which
are helpful to an understanding of their effect on the measurements. As can
be seen, most categories are corrected for in the background subtraction. Ca-
tegories 7 and 8 need further discussions, however. Upper limits on the effect
described in 7 have been measured. Hockenbury, et al. (4) have reported a value

Table I - TANK BACKGROUNDS

Description	Time Dependent	Accounted for In Background Subtraction
1. Tube Noise and Room Natural Radioactivity including Cosmic Rays	No	Yes
2. Sample Natural Activity (or induced activity)	No	Yes
3. Accelerator Produced Room Background	No	Yes
4. Capture of Incident Neutrons in Sample Holder	Yes	Yes
5. Scattered Neutrons Moderated in Tank and Captured in Tank or Sample	No	Yes
6. Capture in Sample of Overlap Neutrons	Yes	Yes
7. Sample Scattered Neutrons Promptly Captured	Yes	No
8. Scattered Neutrons Scattered Back into Sample and Captured	Yes	No

of 1 part in 10^5 for the ratio of scattered neutron effect to capture effect near 80 keV neutron energy for the RPI tank. Recently at Karlsruhe, we have obtained upper limits of 1 part in 5.5 x 10^4 and 1 part in 3.3 x 10^4 at 530 ± 30 keV and 345 ± 28 keV neutron energies, respectively. These values were derived from observation of the gamma ray yields from a gold sample and a carbon scattering sample using thin ^{7}Li targets for the neutron production. Although extrapolation of these values to energies below 100 keV using known cross sections of targets and tank construction materials indicates that this effect is less than 2 %, it is expected that further measurements will be made to try to obtain a better limit. As for the effect described in 8, it is at present very difficult to derive an experimental limit; however, since this requires two scatterings and the through hole is constructed of very thin walled (1 mm) aluminum, and sample holders are also of thin material it is expected that this effect is not significant. Certainly it should be very much smaller than the multiple scattering effect within the target.

3.2 Capture Yield

The time of flight spectra corresponding to the twelve pulse height windows were examined and spectra were summed over the region of pulse heights which gave the best statistical accuracy for the capture effect in each sample. In the case of the gold sample a region from 2.7 MeV gamma-ray energy to just above the neutron binding energy was selected, whereas for ^{59}Co the "hardness" of the pulse height response dictated that the region from 3.4 MeV gamma-ray energy to just above the neutron binding energy of cobalt should be used. Then, corresponding regions in the carbon spectra were added and the capture yield per nucleon for each time channel was computed from the relation:

$$"\sigma_\gamma" = \frac{(C_X - C_{SX})}{(C_A - C_{SA})} \times \frac{N_A}{N_X} \times \frac{\varepsilon_A}{\varepsilon_X} \times \sigma_{\gamma A}$$

where C_X, C_A are the ^{59}Co and gold counts, respectively, C_{SX}, C_{SA} the respective backgrounds, N_X, N_A the ^{59}Co and gold sample thicknesses in nuclei per cm^2, ε_X, ε_A the spectrum fractions for ^{59}Co and gold, and $\sigma_{\gamma A}$ the gold capture cross section. The gold capture cross section given in reference (3) was used in the present measurements.

After subtraction of the carbon counts from the sample spectra, a small
residual background was also subtracted. This residual background was
determined from the region of time just before the onset of the fastest
neutrons and was a constant for each sample. The spectrum fractions were
determined for each sample from an "average" pulse height spectrum obtained
by summing the original two-dimensional data over a number of time channels
and subtracting the appropriate background. The spectrum fraction is the
number of counts in the energy region used for the yield calculation divided
by the total counts. To obtain the total counts the "average" spectra must
be extrapolated to zero gamma-ray energy from the lower threshold of 2 MeV.
Liberal relative uncertainties of 9 % for cobalt and 5 % for gold were
assigned for the spectrum fractions to include the effect of the uncertainty
in this extrapolation. An uncertainty of 6 % was ascribed to the gold
cross section. The capture yields vs. energy are listed in the CCDN file[†]
along with the statistical and total estimated uncertainties.

The resulting capture yield per nucleon is plotted in Figures 1-3
for each channel vs. neutron energy. Energies were calculated from the
measured flight path and the time of each channel relative to the position
of the "prompt" gamma-ray peak from the lithium target. Corrections were
applied for the finite time of flight of the photons and for the non-linearity
of the time analysis system. Where shown, the error bars represent the
uncertainties due to counting statistics only. The total cross section data
of reference (1) have been replotted and appear in the lower part of Figures
1 and 2 in order to clearly show corresponding resonances in the two measure-
ments. The center spectra of these two figures show background subtracted
gamma counts in a 4-8 MeV window taken concurrently with the capture yield
data and with twice as many time channels. These data were useful in establish-
ing resonance energies more accurately and in more clearly defining close
lying resonances. Due to the much greater number of resonances observed in
capture than were observed in the total cross section, the establishment of
a precise energy scale in the present data was very important to the derivation
of the resonance capture widths.

3.3 Radiation Width Analysis

The last phase of data reduction consists of area analysis of the
resolved resonances. For ideally thin targets the area under the capture
yield per nucleon curve for a resonance is proportional to $g\Gamma_n\Gamma_\gamma/\Gamma$, where

[†] Neutron Data Compilation Center, B.P. 9, F-91190 Gif-sur-Yvette, France

g is the statistical factor, Γ_n, Γ_γ, and Γ are the neutron, radiation
and total widths, respectively. For resonances whose spin and neutron
widths have been determined, the capture data can be analysed for the
total radiation width. In cases where spins were not assigned but the
product $g\Gamma_n$ is available, $g\Gamma_\gamma$ may be derived from the capture area data.
The sample used for the ^{59}Co capture measurement was not ideally thin
for scattering. Hence, elaborate multiple scattering and resonance self-
protection calculations were necessary in the treatment of the area
data. These were carried out by means of the FORTRAN IV program, TACASI, (5).
This program also can be used for cases where nearby resonances affect the
capture yield in the resonance of interest through their influence on
the multiple scattering and resonance self-protection. This property was
of particular importance for the ^{59}Co capture due to the high density of
resonances observed. For example the region near 22 keV neutron energy contains
two, relatively broad, s-wave resonances of opposite spin and in addition
several narrow, probably $\ell > 0$ resonances.

The radiation widths obtained for the two broad resonances when
treated together with the four superposed narrow effects differed very
significantly from those obtained by treating the resonances independently.
The region 23.5 - 26.5 keV neutron energy is also complicated by the fact
that two broad resonances are relatively close together. Figure 4 shows
an enlargement of this region with capture yield data points and estimated
total uncertainties. The solid line in this figure is the shape function
computed by TACASI. The total cross section data show three s-wave resonances
in this region: at 24.46 keV with Γ_n = 360 eV, 25.12 keV with Γ_n = 195 eV
and 25.96 keV with Γ_n = 17 eV. However, it is clear from Figure 4 that the
24.42 keV effect seen in capture is too narrow to be simply the 360 eV wide
resonance reported from total cross section measurements, (the experimental
resolution may here be seen to be the ≃185 eV FWHM of the narrow 25.96 keV
resonance).Hence it was postulated that an additional narrow level at about
24.4 keV energy is superposed on the broad s-wave level at this energy; in
addition there is a narrow resonance at 24.7 keV which is partially resolved
in the capture measurement. A second possibility is that the 360 eV wide
resonance at 24.4 keV reported in references (1,2) is in reality an unresolved
doublet with components of almost equal width at 24.4 and 24.7 keV. This does
not seem as probable due to the very high resolution of these total cross

section data. From the kinematics of the elastic scattering, it may be
seen that the presence of the broad level at 24.4 keV must affect the
capture yield in the 25.1 keV resonance by increasing the multiple scattering
effect of the latter (i.e. the higher resonance can "down" scatter into
the lower resonance and thereby contain enhanced second chance capture).
This effect has been corrected for by treating all the resonances together
in this region in deriving the radiation width of the 25.1 keV resonance.
As can be seen from Figure 4, the fit produced by TACASI is quite good.

A summary of the results of the capture analysis is given in Tables
II and III. Spin assignments and values of Γ or $g\Gamma_n$ used in the analysis
were taken from (2). The last column in Table II gives the magnitude
of the multiple scattering correction. In some instances this is seen to
be quite appreciable even though the sample was only 1 mm in thickness.
It should be pointed out also that the 27.3 keV peak observed in capture
appears to be too broad and the 30 keV peak is slightly shifted in energy
with respect to the corresponding resonance in the total cross section
measurement. The 30 keV peak also appears to be asymmetric. This may
mean that these resonances are doublets although they were analyzed as
single resonances. For resonances with unknown g and Γ_n, Table III gives
values of $g\Gamma_n\Gamma_\gamma/\Gamma$ which were derived from the areas under the capture
yield curve.

4. DISCUSSION

The present results on the radiation widths for neutron capture in
^{59}Co are in relatively good agreement with those reported by Moxon (6), in
the energy region 6 - 18 keV if account is taken of a number of doublets
which were not resolved in the work of reference (6). This latter experiment
was carried out under the quite different experimental conditions of linac
produced neutrons and a Moxon-Rae detector.

Average values of the radiation widths have been computed for the
s-wave resonances from the data of Table II. It was found that for seven
J = 3 levels, $\bar{\Gamma}_\gamma$ = 0.564 $\pm$ 0.024 eV, for ten J = 4 levels, $\bar{\Gamma}_\gamma$ = 0.486 $\pm$ 0.016 eV,
and for thirteen additional levels with unassigned spins $\overline{2\,g\Gamma_\gamma}$ = 0.349 $\pm$ 0.013
eV. Natural spreads of 0.091 eV and 0.063 eV were calculated for the J = 3
and J = 4 levels respectively, corresponding to chi-square distributions with

9

Table II

E_0 (keV)	J Ref.(2)	$2 g \Gamma_n$ (eV) Ref.(2)	Γ_n (eV) Ref.(2)	$2 g \Gamma_\gamma$ (eV)	Γ_γ (eV)	% Multiple Scattering
6.38		1.9		0.27 ± 0.04		0.5
8.05	3		38		0.22 ± 0.05	6.8
8.76		0.72		0.25 ± 0.04		–
9.70		2.1		0.42 ± 0.05		–
10.70	4		65		0.30 ± 0.04	8.1
11.87		2.2		0.22 ± 0.03		0.5
13.28	4		20		0.39 ± 0.04	1.8
15.64	3		70		0.64 ± 0.06	3.4
16.98	4		168		0.40 ± 0.04	8.1
19.78		2.3		0.23 ± 0.03		–
22.01	3		700		0.57 ± 0.07	21.0
22.53	4		270		0.35 ± 0.04	12.0
24.44	3		330		0.64 ± 0.07	10.0
25.17	4		180		0.40 ± 0.05	4.0
25.96	4		20		0.65 ± 0.05	1.4
27.28	4		170		0.62 ± 0.04	4.0
29.42		10		0.40 ± 0.04		0.4
30.02	4		320		0.59 ± 0.05	7.7
31.38	3		150		0.47 ± 0.04	2.1
31.84		8.5		0.42 ± 0.04		0.1
32.8	3		130		≈0.59	1.6
33.1	4		40		≈0.56	0.8
34.69		5		≈0.30		
35.0	4		250		≈0.60	3.1
35.53		4.4		0.40 ± 0.04		
36.9		19		0.53 ± 0.10		
40.3		20		0.39 ± 0.04		
40.8		3		0.31 ± 0.03		
41.55		34		0.29 ± 0.03		
43.8		2.4		0.41 ± 0.04		
45.25		≈300				
46.0		270				
56.35	3		210		0.82 ± 0.08	

Table III

ADDITIONAL RESONANCES

E_0 (keV)	$g\Gamma_n\Gamma_\gamma / \Gamma$ (eV)
8.63	0.045 ± 0.011
9.44	0.058 ± 0.011
10.81	0.135 ± 0.02
12.07	0.05 ± 0.01
13.65	0.10 ± 0.01
18.67	0.151 ± 0.015
19.17	0.11 ± 0.01
20.89	0.155 ± 0.016
21.33	0.098 ± 0.010
22.72	0.056 ± 0.010
23.10	0.076 ± 0.008
24.42	$\simeq 0.22$
24.72	$\simeq 0.15$
28.07	0.094 ± 0.011
32.30	
36.23	0.11 ± 0.01
37.4	0.18 ± 0.04
39.59	0.18 ± 0.02
42.81	Multiplet
47.6	Multiplet
49.50	

$\nu \simeq 22$ and $\nu \simeq 32$ degrees of freedom. These values are consistent with the observation(7) that some 34 primary transitions carry approximately 64 % of the strength in neutron capture in the $J^{\pi} = 4^{-}$, 132 eV level of ^{59}Co and approximately 67 % of the strength is accounted for by 40 transitions in thermal neutron capture where both spin states contribute.

The radiation widths for s-wave resonances of Table II were also tested for each spin state for possible correlations with the reduced neutron widths given in reference (2).Positive correlations of this type are evidence for channel capture effects related to particular initial state configurations (valency neutron hypothesis, doorway state formation) or final state configurations (direct capture). Such a correlation has been reported for resonances in a group of other nuclei in this mass region (8), and in particular for the target nucleus ^{60}Ni (9) which has the same neutron number as and not greatly differing neutron separation energy from ^{59}Co. Evidence supporting a direct component in capture of eV neutrons in ^{59}Co has been presented in reference (7). However, for the keV neutron capture, no significant correlation of the type mentioned above is found for either spin state. On the other hand, the present data show a positive value of the capture cross section in the non-resonant regions below 20 keV neutron energy. Pulse height spectra for the off-resonance energy regions 6.4 - 7,9 keV, 9.8 - 10.6 keV, 11.0 - 11.7 keV, 12.2 - 13.0 keV, 13.8 - 15.5 keV and 17.3 - 18.4 keV all show clearly the "hard" gamma-ray spectrum and appropriate high energy cut-off that is characteristic of ^{59}Co capture. Computations with TACASI, which included the relatively large multiple scattering effect for the 1 mm thick target ($\simeq 140$ %), show that this "background" component is not due to the broad 4.3 keV and 5.0 keV resonances. This suggests the possibility of numerous missed small resonances or perhaps a direct capture component.

From the standpoint of astrophysics the capture cross section of ^{59}Co is of interest in the calculation of elemental abundances expected on the basis of neutron capture starting from ^{56}Fe seed material (9). Thus the average cross sections in a Maxwellian neutron flux with several

reasonable values of kT have been computed according to the formula given in reference(10) and are presented in Table IV. The thermal cross section and resonance parameters below 6 keV neutron energy were taken from BNL-325 supplement. Values of the resonance parameters from Table II and reference (2) were used from 5 to 42 keV and above 42 keV the present values of capture yields were included to 200 keV. The resulting value of the Maxwellian averaged cross section for kT = 30 keV is a factor of two larger than that given in reference(10) and should have a marked effect on computed abundances, particularly for the relative abundance of ^{60}Ni. However, the capture cross section of ^{58}Fe is needed to make quantitative predictions.

5. ACKNOWLEDGEMENTS

13

Table IV   Maxwellian Averaged Capture Cross Sections

kT (keV)	10	20	30	40	50	60	70
$<\sigma>$(mb)	141	92	72	61	53	47	42

REFERENCES

(1)   J.B. GARG, J. RAINWATER and W. W. HAVENS, Jr., in BNL
        325 Supplement No. 2.

(2)   J. MORGENSTERN, S. de BARROS, G. BIANCHI, C. CORGE,
        V. D. HUYNH, J. JULIEN, G. le POITTEVIN, F. NETTER, and
        C. SAMOUR, Intern. Conf. on the Study of Nuclear Structure
        with Neutrons, Antwerp, Paper 86 (1965).

(3)   D. KOMPE , Nucl. Phys. A 133 (1969) 513.

(4)   R.C. BLOCK and R.W. HOCKENBURY,CONF-701002 (1971)   355.

(5)   F.H. FRÖHNER, General Atomic Report GA-6906 (1966).

(6)   M.C. MOXON, International Conf. on the Study of Nuclear Structure
        with Neutrons, Antwerp, Paper 88 (1965).

(7)   O.A. WASSON, R.E. CHRIEN, M.R. BHAT, M.A. LONG, and M. BEER,
        Phys. Rev. 176 (1968) 1314.

(8)   R.G. STIEGLITZ, R.W. HOCKENBURY and R.C. BLOCK,
        Nucl. Phys. A 163 (1971) 592 .

(9)   H. BEER and R.R. SPENCER, (to be published).

(10)   A comprehensive review is given by B.J. ALLEN, J.H. GIBBONS,
        and R.L. MACKLIN, Advances in Nuclear Physics, Vol. 4, Plenum
        Press, New York, (1971) 205.

FIGURE CAPTIONS

Fig. 1: (Top) - Capture yield $\underline{vs.}$ neutron energy for ^{59}Co in the energy region 6-25 keV.

(Middle) - Gamma-ray counts $\underline{vs.}$ neutron energy with twice the number of time channels as above.

(Bottom) - Total neutron cross section of ^{59}Co.

Fig. 2: (Top) - Capture yields $\underline{vs.}$ neutron energy for ^{59}Co in the energy region 25-100 keV.

(Middle) - Gamma-ray counts $\underline{vs.}$ neutron energy with twice the number of time channels as above.

(Bottom) - Total neutron cross section of ^{59}Co.

Fig. 3: Capture yield $\underline{vs.}$ neutron energy for ^{59}Co in the energy region 100 - 200 keV.

Fig. 4: Expanded view of the capture yield in the neutron energy region 24-26 keV showing the fit obtained from the program TACASI (solid line).
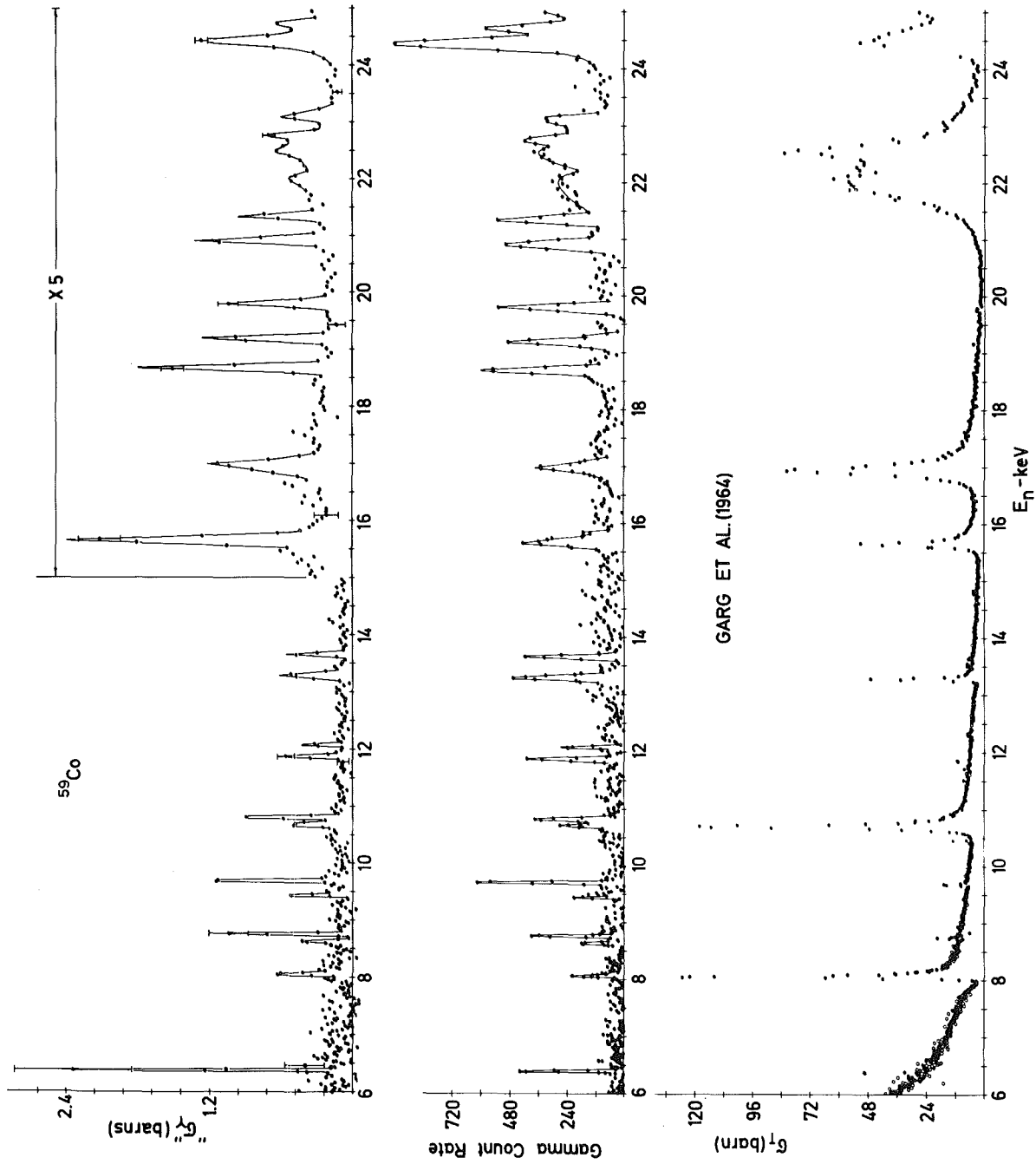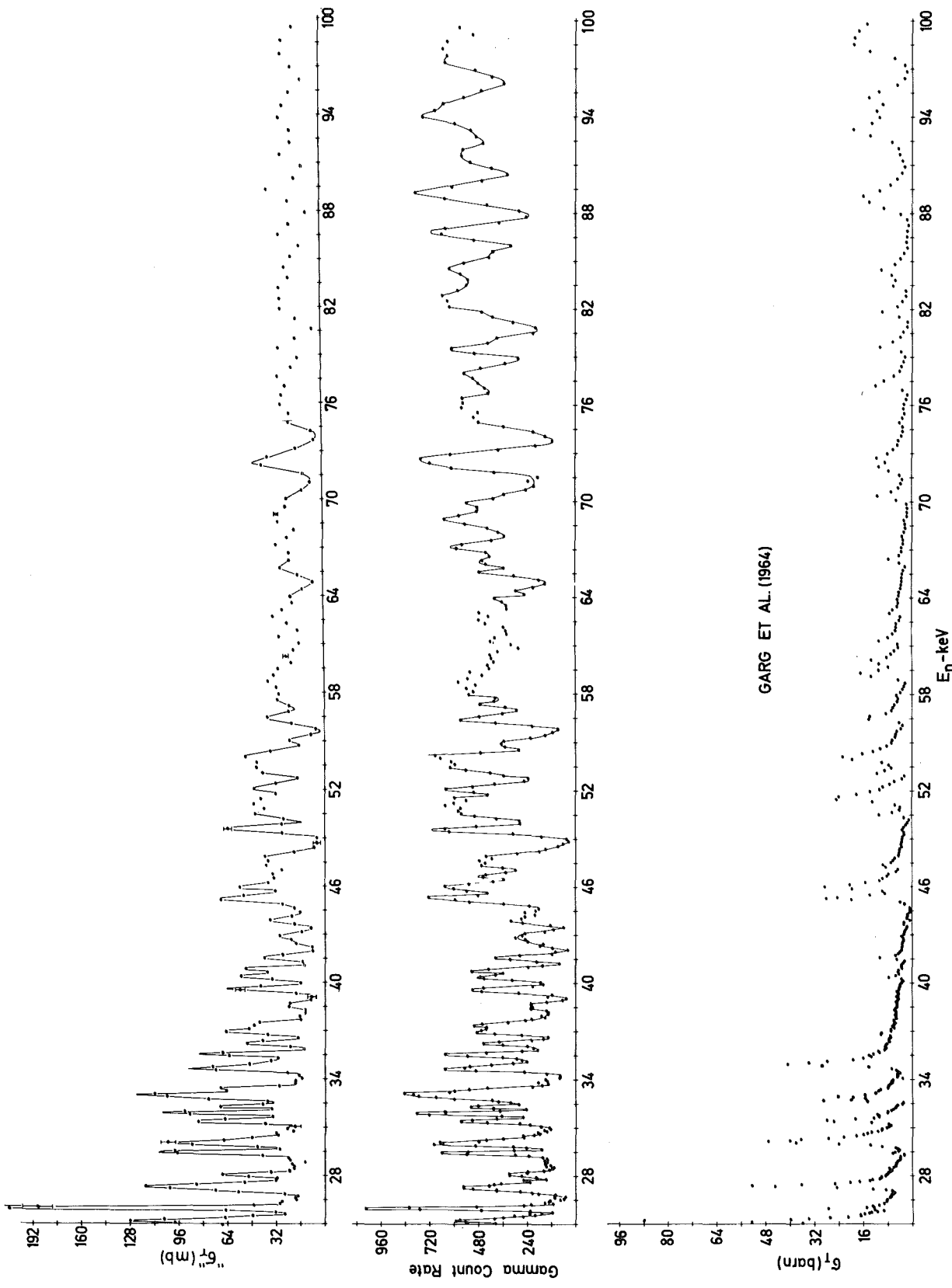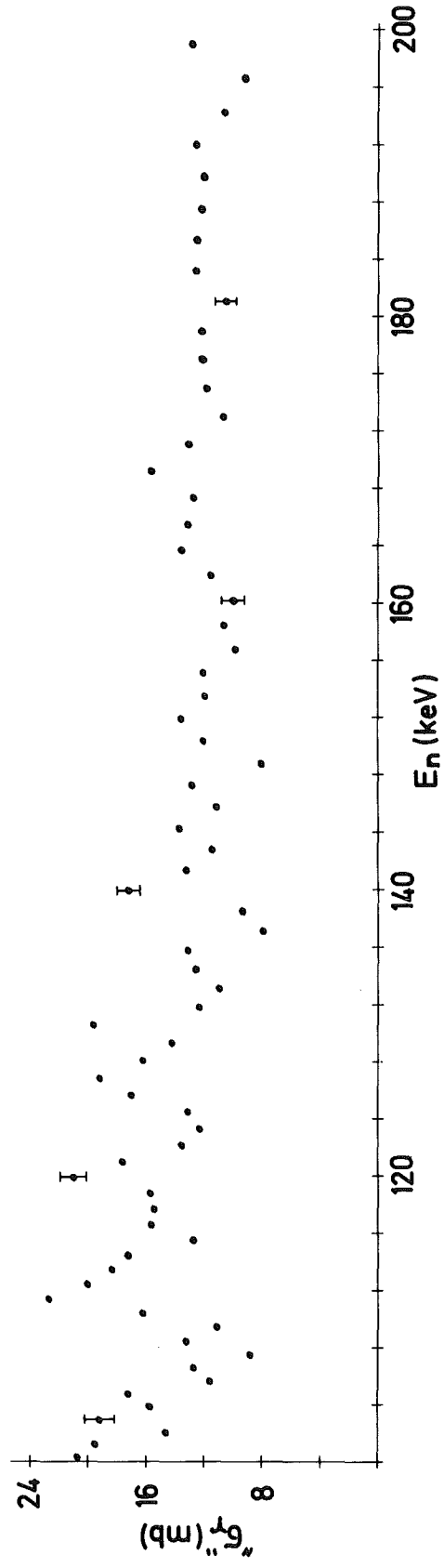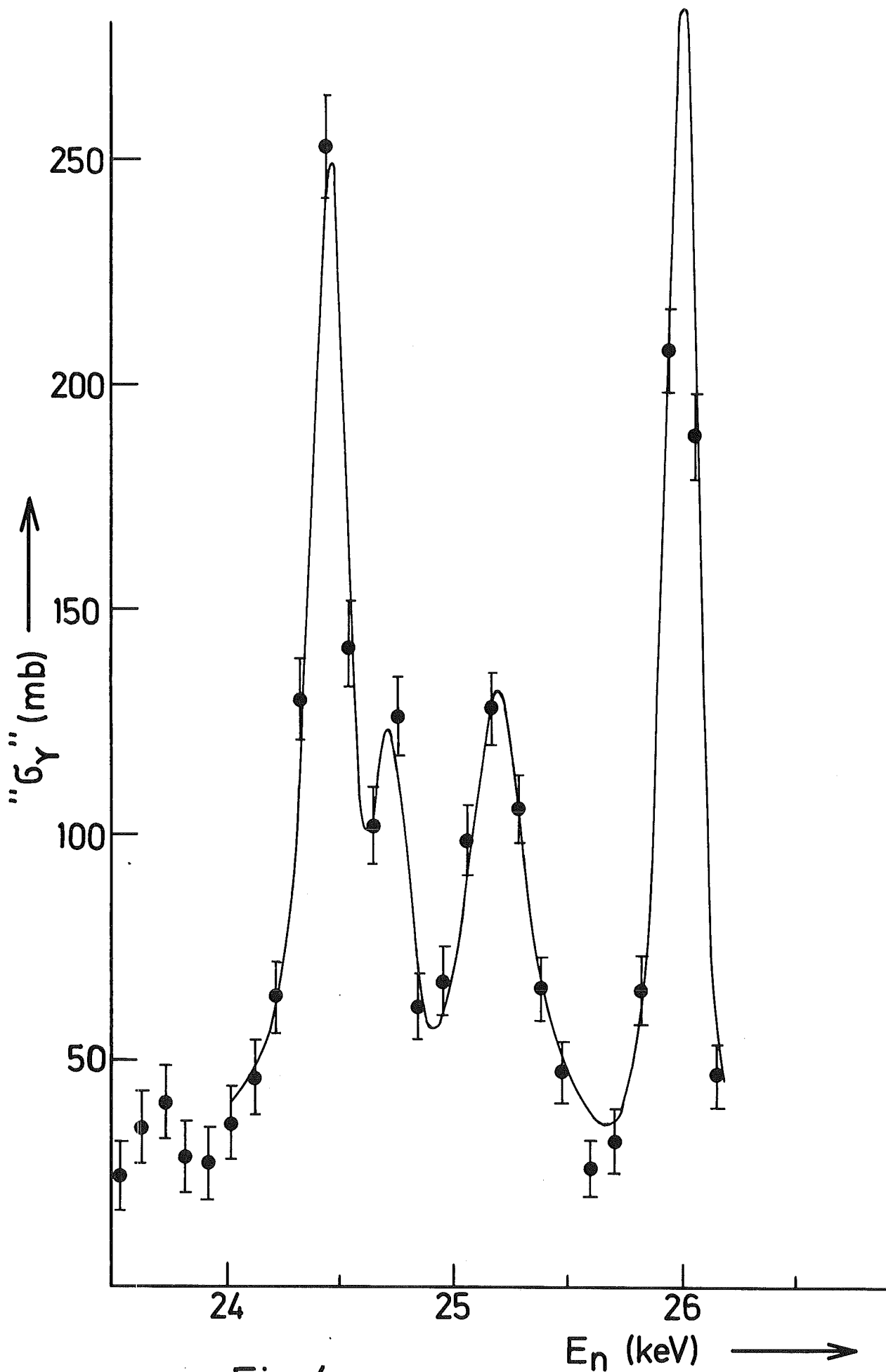
Fig.1

GARG ET AL. (1964)

Fig.2

Fig.3

Fig.4